energy&fuels

pubs.acs.org/EF Article

Evaluation of Methane Dynamic Adsorption−Diffusion Process in Coals by a Low-Field NMR Method

Zhentao Li, Dameng Liu,* Songbin Xie, Xianglong Fang, Guangyao Si, Yidong Cai, and Yunpeng Wang

Cite This: *Energy Fuels* 2020, 34, 16119−16131 Read Online

ACCESS | Metrics & More | Article Recommendations

ABSTRACT: Quantitative characterization of multiphase methane and investigation of the methane dynamic adsorption process of coals were performed by a low-field nuclear magnetic resonance (NMR) method. Meanwhile, methane diffusion behaviors during the step-by-step pressurization adsorption process were evaluated by three diffusion models. The results indicate that the transverse relaxation time (T_2) spectra of methane demonstrate two distinct peaks of adsorbed methane (P1, T_2 < 2.5 ms) and porous medium-confined methane (P2) at a low-pressure step (∼1.0 MPa), and the third peak of bulk methane (P3) obviously appears when the pressure >2.0 MPa. The integrated T_2 amplitude of adsorbed methane increases quickly during the first 2 h (>75% of total) and then gradually reaches a maximum value in the last 4 h during the initial pressure step of ∼1.0 MPa, whereas it reaches >90% of total amplitude in 1 h as the pressure is increased step-by-step. According to the strong linear relationship between the adsorbed methane volume and the integrated T_2 amplitude, the real-time methane adsorption volume can be determined, and adsorption isotherms from the NMR method are found to be mostly overlapped with those of the volumetric method. Moreover, the effective diffusion coefficient of the unipore model (10^{-6} to 10^{-5} s^{-1}) coincides with the micropore diffusion coefficient of the bidisperse model and the slow diffusion coefficient of the multiporous model, which is generally 1−3 orders of magnitude less than the macropore diffusion coefficient (10^{-3} to 10^{-2} s^{-1}) and the fast diffusion coefficient (10^{-2} s^{-1}) or transitional diffusion coefficient (10^{-4} to 10^{-3} s^{-1}). The dynamic changes in diffusion parameters with pressure may be related to the comprehensive effects of methane diffusion mechanisms and coal matrix swelling under different adsorption pressures.

1. INTRODUCTION

Coalbed methane (CBM), which is found mainly adsorbed on a coal matrix pore surface with its main component being methane (80−90%) and the rest impurity gases, has attracted the great attention of many countries because of its great significance for mining safety, greenhouse gas reduction, and solving the supply−demand contradiction of natural gases.[1−3] The gas adsorption kinetics in a coal reservoir is a comprehensive dynamic process involving the gas seepage stage, bulk diffusion stage, surface diffusion stage, and gas adsorption stage,[4,5] and the gas adsorption capacity is one of the key parameters for accurately predicting the gas-in-place content and gas production behaviors.[6−8] Commonly, the gas adsorption process and the capacity of coals are determined by the volumetric and gravimetric methods.[9,10] Based on the gas isothermal adsorption analysis of coals, it has been reported that the gas adsorption behavior and capacity are primarily dominated by the coal rank, maceral composition, moisture content, pore structure, temperature, pressure, and so forth.[11−15] Moreover, the gas diffusion process in coals can be accurately described by the unipore model, the bidisperse model, and the multiporous model with fitting gas adsorption rate data, which mainly depend on the pore size/volume distribution of coals.[16,17] These results indicate that the gas diffusion behavior in the pore network plays an important role in controlling the gas adsorption process. Therefore, the understanding of the gas dynamic adsorption−diffusion process in the coal matrix is key to reveal the CBM storage mechanism and enhance the CBM recovery.

A significant amount of studies have verified that the low-field nuclear magnetic resonance (NMR) technique is an efficient and nondestructive method for characterizing the pore structure, porosity, permeability, surface wettability, and gas−water two-phase flow behaviors of unconventional reservoirs.[18−23] Recently, there have been some studies that begun to use the low-field ^{1}H NMR relaxation characteristics to make qualitative and quantitative analyses of multiphase methane gases in coal and shale. By analyzing the ^{1}H NMR wide-line spectra and transverse relaxation time (T_2) spectral characteristics of methane phases in coals, Alexeev et al.[24] and Guo et al.[25] found that methane exhibits three phase states (adsorbed state on the surface of small pores, free state in large pore fractures, and solid-solution state in the coal matrix) in the open/closed pore-fracture system and solid solutions of coals, corresponding to the adsorbed methane peak, porous medium-confined methane peak, and bulk methane peak in the T_2 spectrum. Based on the independently developed low-field

Received: September 20, 2020
Revised: November 16, 2020
Published: December 3, 2020

https://dx.doi.org/10.1021/acs.energyfuels.0c03168
Energy Fuels 2020, 34, 16119−16131

Table 1. Sampling Information and Results of $R_{o,m}$, Maceral Composition, and Proximate Analysis of Coal Samples[a]

			Coal composition (%)				Proximate analysis (%)			
Sample no.	Sampling location	$R_{o,m}$ (%)	Vitrinite	Inertinite	Liptinite	Mineral	M_{ad}	A_{ad}	V_{ad}	FC_{ad}
LRC	Southern Junggar Basin	0.64	55.6	39.8	3.2	1.4	5.54	4.65	33.46	56.35
MRC	Northwestern Qinshui Basin	1.68	69.3	20.1	0	10.6	0.84	14.6	20.74	63.82
HRC		2.61	74.5	14.2	0	11.3	0.67	17.6	13.6	68.13

[a]Note: M_{ad} - Moisture content (wt %, air dry basis), A_{ad} - ash yield (wt %, air dry basis), V_{ad} - volatile matter (wt %, air dry basis), and FC_{ad} - fixed carbon (wt %, air dry basis).

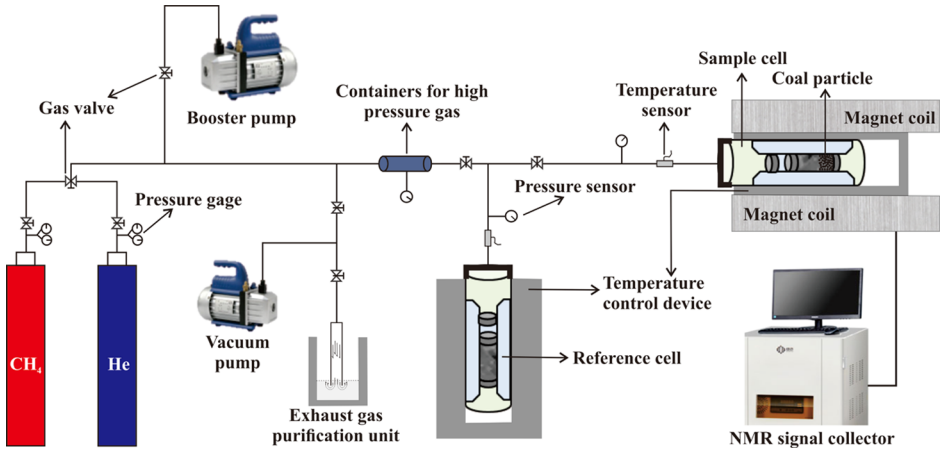

Figure 1. Schematic diagram of the low-field NMR experimental setup (modified from Zheng et al.,[34] Copyright © 2020, American Chemical Society).

NMR gas adsorption experimental setup, Yao et al.[26] proposed a quantitative method to assess the methane adsorption capacity of coals using the T_2 amplitude of coal-adsorbed methane, which shows very good agreement with the results of traditional volumetric method under the same experimental conditions. Meanwhile, the gas adsorption capacity and the specific contents of free gas and adsorbed gas in shale can also be accurately quantified by the corresponding T_2 spectral distribution from low-field NMR measurements.[27] Some researchers studied the influence of adsorbed/nonadsorbed water on methane adsorption/desorption process of coals using NMR spectral measurements and found that the water film in pore walls and the water droplet near the pore throat can seriously reduce or block the methane adsorption/desorption process on the micropore.[28−30] Zhao and Wang[31] and Liu et al.,[32] by studying the effect of CO_2 injection on the methane adsorption process in shale with the NMR-based methodology, observed that the methane adsorbed onto the shale pore surface can be strongly replaced by CO_2 and then only the desorbed methane changes to the free-state methane in the pore center and is hardly gets extracted from organic pores. Furthermore, Quan et al.[33] utilized the low-field NMR technology to study the methane desorption−diffusion dynamics of coals and discovered that the dynamic variation of the methane diffusion process caused by the pore deformation behavior is related to different desorption characteristics under the conditions of various depressurization schemes.

However, the above-stated research mainly concentrates on the application of the NMR-based technology in the identification of multiphase methane gases, quantitative characterization of gas adsorption capacity, and its influencing factors in coal or shale gas reservoirs. There is no further analysis on the gas dynamic adsorption−diffusion process and the control mechanisms of gas diffusion behavior in coal and shale. In this work, a series of step-by-step CH_4 pressurization adsorption measurements with a temperature of 25 °C were conducted on different rank coals using the low-field NMR instrument to evaluate the CH_4 dynamic adsorption−diffusion process. During the step-by-step pressurization adsorption process, the NMR T_2 spectral distribution of multiphase methane (adsorbed methane and free methane) was continuously recorded by distinguishing the ^1H protons of methane in coals. Meanwhile, the amounts of adsorbed methane and free methane were quantitatively calculated by the linear relationship between the methane volume and their corresponding T_2 amplitudes, respectively. Compared with the Langmuir parameters obtained from the volumetric method, the application of the NMR-based adsorption method was further verified and the CH_4 dynamic adsorption process could be characterized by the dynamic change in the T_2 spectra. Moreover, three different diffusion models (unipore, bidisperse, and multiporous models) were applied to calculate the CH_4 diffusion parameters of coals using the integrated T_2 amplitudes with respect to different CH_4 pressurization stages. Finally, this study also discussed the dynamic changes in diffusion parameters and their controlling mechanisms with increasing adsorption pressure.

2. SAMPLES AND METHODS

2.1. Sampling and Coal Analyses. According to Chinese Standard Method GB/T 23561.1-2009, three fresh bulk coal samples (~15 × 15 × 15 cm^3) used in this study were collected from active underground mines in the southern Junggar Basin and northwestern Qinshui Basin of China, respectively. Based on the Leitz MPV-3 photometer microscope, the maximum vitrinite reflectance ($R_{o,m}$) and maceral composition analyses were performed on polished coal slabs (~3 × 3 cm^2) under the guidance of China National Standards of GB/T 6948-2008 and GB/T 8899-2013. Moreover, the proximate

https://dx.doi.org/10.1021/acs.energyfuels.0c03168
Energy Fuels 2020, 34, 16119−16131

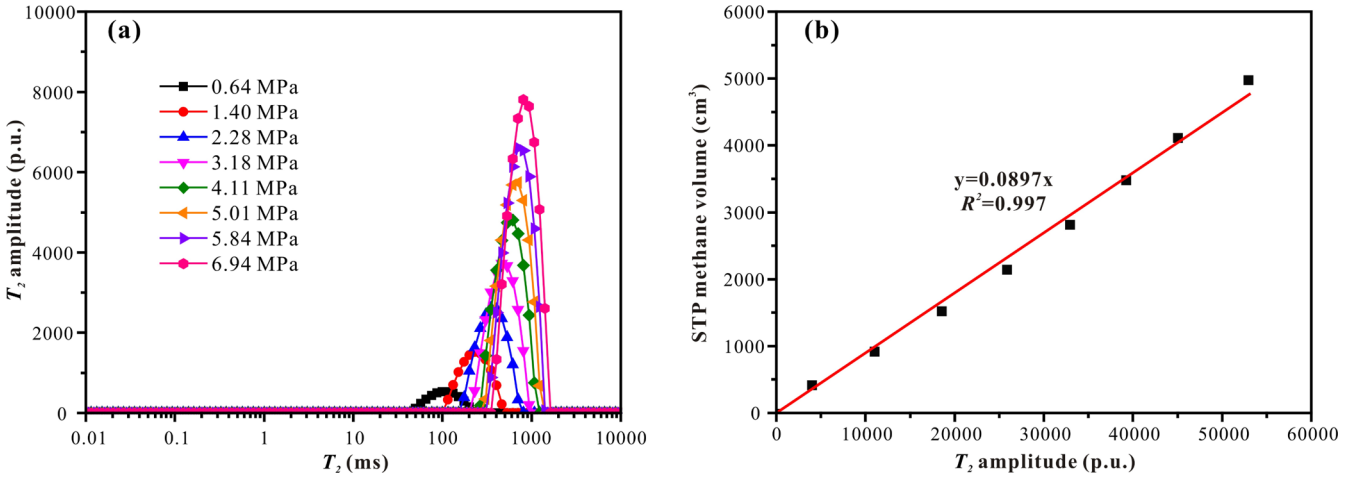

Figure 2. T_2 spectral distribution of bulk methane of different pressures (a) and the linear correlation between the STP free methane volume and the total T_2 amplitude (b).

analysis of coal samples was analyzed by the Automatic Proximate Analyzer 5E-6600. The detailed experimental procedures of these measurements were in accordance with our previous work.[17] The results of $R_{o,m}$, maceral composition, and proximate analysis of coal samples are summarized in Table 1, indicating that the coal sample collected from the southern Junggar Basin belongs to low-rank coal (LRC) with an $R_{o,m}$ of 0.64%, whereas a medium-rank coal (MRC) with an $R_{o,m}$ of 1.68% and a high-rank coal (HRC) with an $R_{o,m}$ of 2.61% originated from the northwestern Qinshui Basin.

2.2. Experimental Procedure and Method. The low-field NMR measurements of methane adsorbed on coals were performed on the Niumag MiniMR-60 analytical instrument with a constant magnetic field of 0.54 T and a frequency of 23.15 MHz, which consists of the reference cell, the sample cell, and the high-pressure gas-delivery system (Figure 1). Prior to methane isothermal adsorption measurements, coal samples were crushed and sieved into 60−80 mesh (0.18−0.25 mm) powders, and dried in a vacuum oven at 105 °C for 24 h to remove free water and other impurities. Moreover, both the reference cell and sample cell were put into the thermostatic apparatus at a temperature of 25 °C and preheated for 4 h at least. First, the bulk methane was injected into the reference cell with volume of 70.41 cm^3 under setting pressures and then the corresponding NMR T_2 spectrum was measured to establish the correlation between the T_2 amplitude and the methane volume. Subsequently, the dried powder sample was weighed and placed into the sample cell and vacuumed for 2 h. The dead volume has been measured and calculated by injecting the helium at a gas pressure of ∼3 MPa before methane adsorption measurements. Finally, the methane was first injected into the reference cell at certain pressure and then entered into the sample cell as the valve opens. During the adsorption process, the change in the NMR T_2 spectrum with time was recorded every 10 min for the first 2 h, after which the recording interval of the NMR T_2 spectrum was increased to 30 min for the next 4 h until the change in T_2 amplitude of two consecutive tests could be neglected. For each sample, the NMR T_2 spectra at six or seven different pressures were recorded by repeating the above procedures.

2.3. Quantitative Calculation Methodology of Multiphase Methane. *2.3.1. Quantification of Free Methane by Low-Field NMR Measurements.* Because of the different magnetic relaxation behaviors of multiphase methane in coals, the free methane (bulk methane and porous medium-confined methane) and adsorbed methane can be identified by different ranges of T_2 relaxation times and their amounts were further calculated with the corresponding T_2 amplitude.[25] In this study, the NMR T_2 spectrum of free methane was determined at 25 °C and a series of pressures (0.64, 1.4, 2.28, 3.18, 4.11, 5.01, 5.84, and 6.94 MPa), indicating that a series of distinct T_2 spectral peaks occur at approximately 50−2000 ms, and the spectral peak increases with the increase of gas pressure (Figure 2a). Yao et al.[26,27] proposed that the NMR T_2 amplitude of free methane is related to the number of ^1H protons and increases linearly with the volume concentration of methane at a constant temperature, as follows

$$V_{free} = C_1 \times T_{2-free} \quad (1)$$

where V_{free} is the free methane volume, which can be calculated by the ideal gas state equation at the STP condition (cm^3); $T_{2\text{-free}}$ is the T_2 amplitude of free methane at a given pressure (p.u.); and C_1 is the slope of the fitting curve. As shown in Figure 2b, there is a significant linear correlation between the STP free methane volume and the total T_2 amplitude ($y = 0.0897x$, $R^2 = 0.997$), indicating that the C_1 value is equal to 0.0897 in this study.

2.3.2. Quantification of Adsorbed Methane by the Volumetric Method and Low-Field NMR. The conventional volumetric method has been widely used to calculate the methane adsorption capacity of coals, which has been comprehensively reported in previous studies.[9,15] In this study, the dead volume (V_d, cm^3) is composed of the volume of the connecting pipeline, the volume between coal particles, and the remaining volume of the sample cell after coal sample loading, which can be determined as follows

$$V_d = \left(\frac{P_0 Z_1}{P_1 Z_0} - 1\right) \times V_r \quad (2)$$

where P_0 is the initial pressure of helium in the reference cell (MPa); P_1 is the equilibrium pressure of helium in the reference cell and the dead space of the sample cell (MPa); Z_0 and Z_1 are the corresponding helium compression factors when the gas pressure is at P_0 and P_1, respectively; and V_r is the volume of the reference cell (70.41 cm^3).

When the methane is injected into the reference cell at a certain pressure (P_i), the total methane volume (V_{it}, cm^3) consists of the free methane volume in the reference cell and the dead space of the sample cell, which can be calculated using the following equation

$$V_{it} = \left(\frac{P_i V_r}{Z_i RT} + \frac{P_{ie-1} V_d}{Z_{ie-1} RT}\right) \times 22.4 \times 1000 \quad (3)$$

where $P_{ie\text{-}1}$ is the last equilibrium pressure of methane in the reference and sample cells (i = 1 to 6/7, MPa); $Z_{ie\text{-}1}$ and Z_i are the corresponding methane compression factors when the gas pressure is at $P_{ie\text{-}1}$ and P_i, respectively; R is the universal gas constant (8.314 J·mol^{-1}·K^{-1}); and T is the temperature (25 °C). Moreover, when the adsorption equilibrium state is reached, the total volume of free methane in the reference cell and the dead space of the sample cell can be expressed as

https://dx.doi.org/10.1021/acs.energyfuels.0c03168
Energy Fuels 2020, 34, 16119−16131

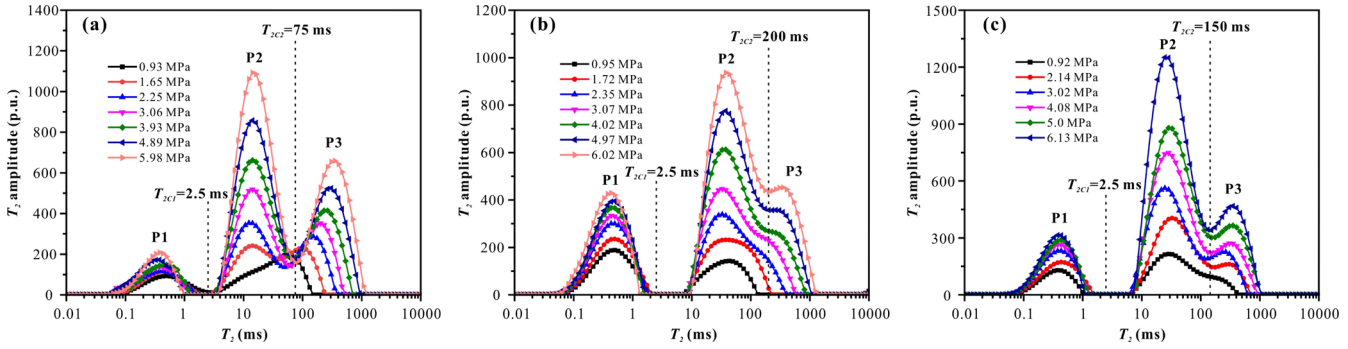

Figure 3. T_2 spectral distribution of multiphase methane in a coal-filled sample cell with respect to different pressures for coal samples. (a): LRC sample; (b): MRC sample; and (c): HRC sample.

$$V_{if} = \frac{P_{ie}(V_r + V_d)}{Z_{ie}RT} \times 22.4 \times 1000 \quad (4)$$

where P_{ie} is the equilibrium pressure of methane (MPa) and Z_{ie} is the corresponding methane compression factor when the gas pressure is at P_{ie}. Therefore, the volume of adsorbed methane at equilibrium pressure P_{ie} can be derived by

$$V_{ia} = \sum_{n=1}^{i} (V_{it} - V_{if} + V_{(i-1)a}) \times 22.4 \times 1000 \quad (5)$$

where V_{ia} is the volume of adsorbed methane at equilibrium pressure P_{ie} (cm^3).

According to the NMR T_2 spectral distribution of coal samples at pressure P_{ie}, the T_2 amplitude of adsorbed methane ($T_{2i\text{-}P1}$) and V_{ia} can also be characterized as a linear relationship

$$V_{ia} = C_2 \times T_{2i-P1} \quad (6)$$

where C_2 is the slope of the fitting curve, which depends on the methane adsorption process of different coal samples.

3. RESULTS AND DISCUSSION

3.1. T_2 Spectral Characteristics of Multiphase Methane in Coals. Figure 3 shows the T_2 spectral distribution of multiphase methane in a coal-filled sample cell under different equilibrium pressure conditions. The results show that the T_2 spectra of different rank coals usually exhibit two distinct peaks of adsorbed methane (P1) and porous medium-confined methane (P2), while another peak of bulk methane (P3) obviously appears when the equilibrium pressure is greater than 2.0 MPa. Herein, the T_2 time of P1 mainly falls within 2.5 ms, which does not change as the equilibrium pressure increases. This phenomenon may be related to the adsorption mechanism between methane molecular and micropore surface of coals.[26] In contrast to P1, the cut-off point of T_2 time (T_{2C2}) between P2 and P3 varies for different rank coals, namely, 75 ms for the LRC sample, 200 ms for the MRC sample, and 150 ms for the HRC sample in this study. Because the P2 peak originated from the relaxation of free-state methane filled into large pores or fractures,[25] its T_2 boundary is primarily dominated by the pore morphology, connectivity, and pore size distribution. As shown in Figure 4, the total T_2 amplitudes of P1, P2, and P3 all increase to varied extents with increasing equilibrium pressure. For adsorbed methane, the total T_2 amplitude of the LRC sample increases sharply in a low-pressure range and then tends to gently increase to an extreme value with increasing pressure (Figure 4a), whereas those of MRC and HRC samples gradually increase to a limiting value as the pressure increases (Figure 4a,b). Moreover, the total T_2 amplitude of the porous medium-confined methane and bulk

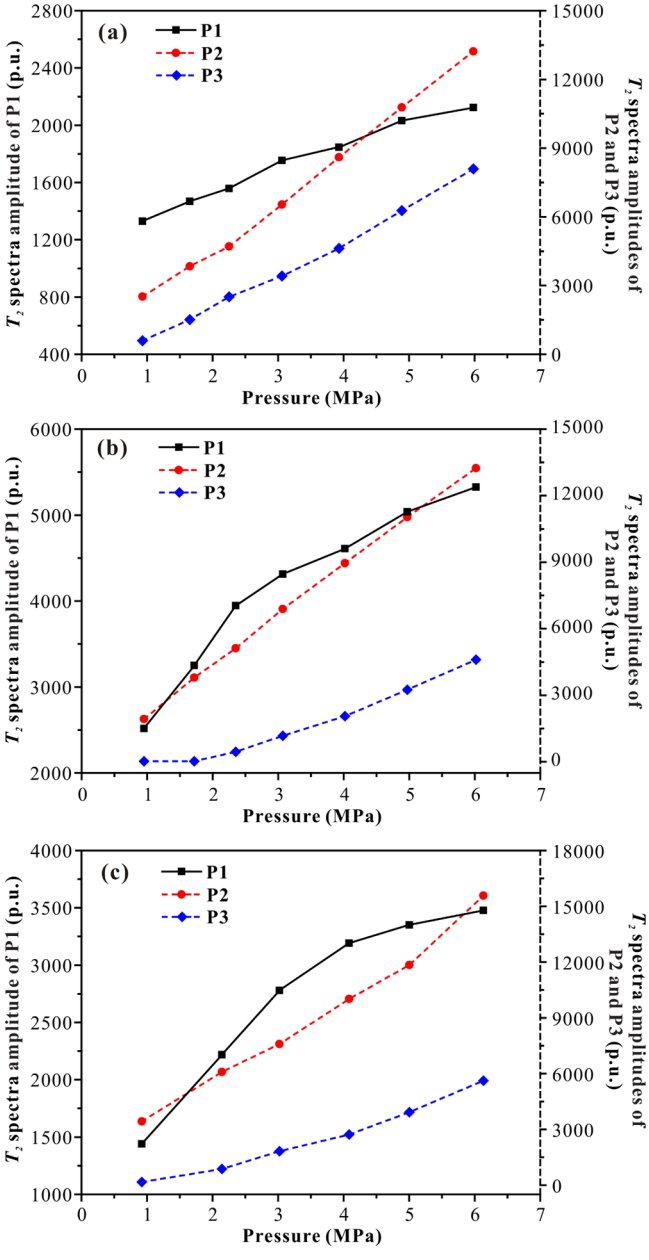

Figure 4. Variation of total T_2 amplitudes for adsorbed methane (P1), porous medium-confined methane (P2), and bulk methane (P3) with increasing pressure. (a): LRC sample; (b): MRC sample; and (c): HRC sample.

https://dx.doi.org/10.1021/acs.energyfuels.0c03168
Energy Fuels 2020, 34, 16119−16131

Table 2. Quantitative Calibration of the Adsorbed Methane Volume of Coal Samples by the Volumetric Method and the Low-Field NMR Method[a]

			Volumetric method						Low-field NMR method		
Sample no.	m (g)	V_d (cm^3)	P_i (MPa)	V_{it} (cm^3)	P_{ei} (MPa)	V_{if} (cm^3)	V_{ia} (cm^3)	V_{VOL} (cm^3/g)	$T_{2i\text{-}P1}$ (p.u.)	V_{NMR} (cm^3/g)	$\lvert V_{NMR}\text{-}V_{VOL}\rvert/V_{VOL}$ (%)
LRC	30.05	35.9	1.55	1013.02	0.93	907.91	105.11	3.50	1329.41	3.89	11.14
			2.04	1651.26	1.65	1631.08	125.29	4.17	1468.19	4.30	3.12
			2.56	2253.52	2.25	2247.48	131.33	4.37	1557.05	4.56	4.35
			3.5	3124.94	3.06	3099.7	156.57	5.21	1753.24	5.13	1.54
			4.38	4052.42	3.93	4040.91	168.08	5.59	1845.9	5.41	3.22
			5.39	5126.48	4.89	5110.38	184.18	6.13	2031.75	5.95	2.94
			6.53	6368.42	5.98	6363.02	189.58	6.31	2123.23	6.22	1.43
MRC	27.91	32.01	1.66	1086.99	0.95	893.79	193.2	6.92	2516.08	7.43	7.37
			2.18	1719.77	1.72	1640.01	272.96	9.78	3249.7	9.59	1.94
			2.7	2312.72	2.35	2265.34	320.34	11.48	3945.03	11.65	1.48
			3.47	3052.46	3.07	2996.48	376.32	13.48	4312.73	12.73	5.56
			4.47	4008.57	4.02	3988.22	396.67	14.21	4610.37	13.61	4.22
			5.41	5023.51	4.97	5010.52	409.66	14.68	5038.93	14.88	1.36
			6.5	6185.05	6.02	6175.05	419.66	15.04	5324.66	15.72	4.52
HRC	27.81	36.1	1.81	1188.3	0.92	899.66	288.64	10.38	1440.59	10.37	0.10
			2.97	2294.36	2.14	2137.49	445.51	16.02	2219.35	15.97	0.31
			3.63	3183.78	3.02	3062.75	566.54	20.37	2778.22	19.99	1.87
			4.69	4273.32	4.08	4213.69	626.17	22.52	3191.52	22.96	1.95
			5.51	5281.39	5.0	5244.69	662.87	23.84	3351.37	24.11	1.13
			6.75	6593.35	6.13	6550.63	705.59	25.37	3477.57	25.02	1.38

[a]*Note: m* - sample weight, V_{VOL} - methane adsorption volume per unit mass sample, as calculated by the volumetric method, and V_{NMR} - methane adsorption volume per unit mass sample, as calculated by the low-field NMR method.

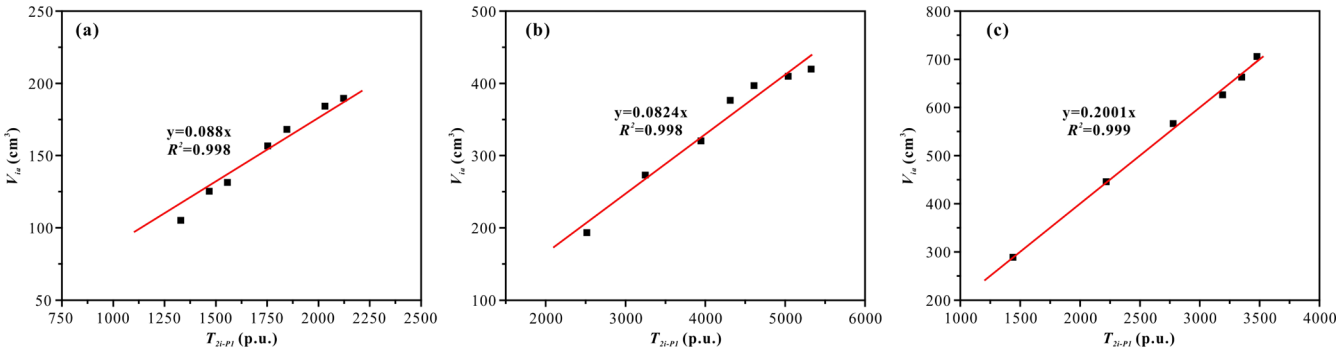

Figure 5. Linear relationship between the T_2 amplitude and the adsorbed methane volume of LRC sample (a), MRC sample (b), and HRC sample (c).

methane almost linearly increases with increasing pressure for different rank coal samples. These phenomena are consistent with the results of Yao et al.,[26,27] where the total T_2 amplitude of adsorbed methane in coals/shales demonstrated a Langmuir function trend with the equilibrium pressure of methane.

3.2. Quantitative Characterization of Adsorbed Methane and Adsorption Isotherms. As discussed above, the porous medium-confined methane volume and the bulk methane volume can be quantified by their corresponding T_2 amplitudes of different pressures using eq 1, respectively. Moreover, the adsorbed methane volumes at different equilibrium pressures can be accurately determined by the volumetric method using eqs 2−5 (Table 2). As shown in Figure 5, a strong linear relationship between the adsorbed methane volume and the corresponding T_2 amplitude (eq 6) has been proven for each coal sample, as follows

$$V_{ia-LRC} = 0.088 \times T_{2i-P1}; \qquad R^2 = 0.998 \tag{7}$$

$$V_{ia-MRC} = 0.0824 \times T_{2i-P1}; \qquad R^2 = 0.998 \tag{8}$$

$$V_{ia-HRC} = 0.2001 \times T_{2i-P1}; \qquad R^2 = 0.999 \tag{9}$$

Based on eqs 7−9, the adsorbed methane volume per unit mass of coal samples (V_{NMR}) can also be calculated using the T_2 amplitude of P1 at different equilibrium pressures (Table 2). For the LRC sample, the V_{NMR} increases from 3.89 cm^3/g at 0.93 MPa to 6.22 cm^3/g at 5.98 MPa, and the relative deviation with respect to the volumetric method is in the range of 1.43−11.14%. Meanwhile, the V_{NMR} of the MRC sample also increases from 7.43 cm^3/g at 0.95 MPa to 15.72 cm^3/g at 6.02 MPa with the relative deviation of 1.36−7.37%. It is found that the deviation between the volumetric method and the NMR method is mainly lower than 5%, whereas it may be significant at a low-pressure adsorption stage (11.14% for the LRC sample and 7.37% for the MRC sample). Moreover, the V_{NMR} of the HRC sample varies from 10.37 cm^3/g at 0.92 MPa to 25.02 cm^3/g at 6.13 MPa with an extremely low relative

https://dx.doi.org/10.1021/acs.energyfuels.0c03168
Energy Fuels 2020, 34, 16119−16131

deviation of 0.1−1.95%. On one hand, partially adsorbed methane distributed for <0.1 ms may be inaccurately measured because the echo spacing is set as 0.3 ms,[26] which may result in the V_{NMR} value being generally low at some pressure stage. On the other hand, the change in the ambient temperature of laboratory and the exothermic adsorption may cause some small fluctuations in the temperature of the sample cell when the NMR instrument records signals. As shown in Figure 6, the NMR methane adsorption isotherms of coal samples are well in accord with the Langmuir equation (R^2 > 0.98), and the corresponding Langmuir volume ($V_{L\text{-}NMR}$) and Langmuir pressure ($P_{L\text{-}NMR}$) are 6.826 cm^3/g and 0.887 MPa for the LRC sample, 19.94 cm^3/g and 1.725 MPa for the MRC sample, and 34.974 cm^3/g and 2.305 MPa for the HRC sample, respectively. Compared with the Langmuir volume obtained from the volumetric method, the $V_{L\text{-}NMR}$ of the LRC sample has a relative deviation of 9.4% (Figure 6a), whereas that of MRC and HRC samples demonstrates the relative deviation <1.0% (Figure 6b,c). These results suggest that the methane adsorption data of coals determined by the low-field NMR measurement are reliable, and this method can be used to investigate the real-time dynamic gas adsorption/desorption and diffusion behaviors of coals.

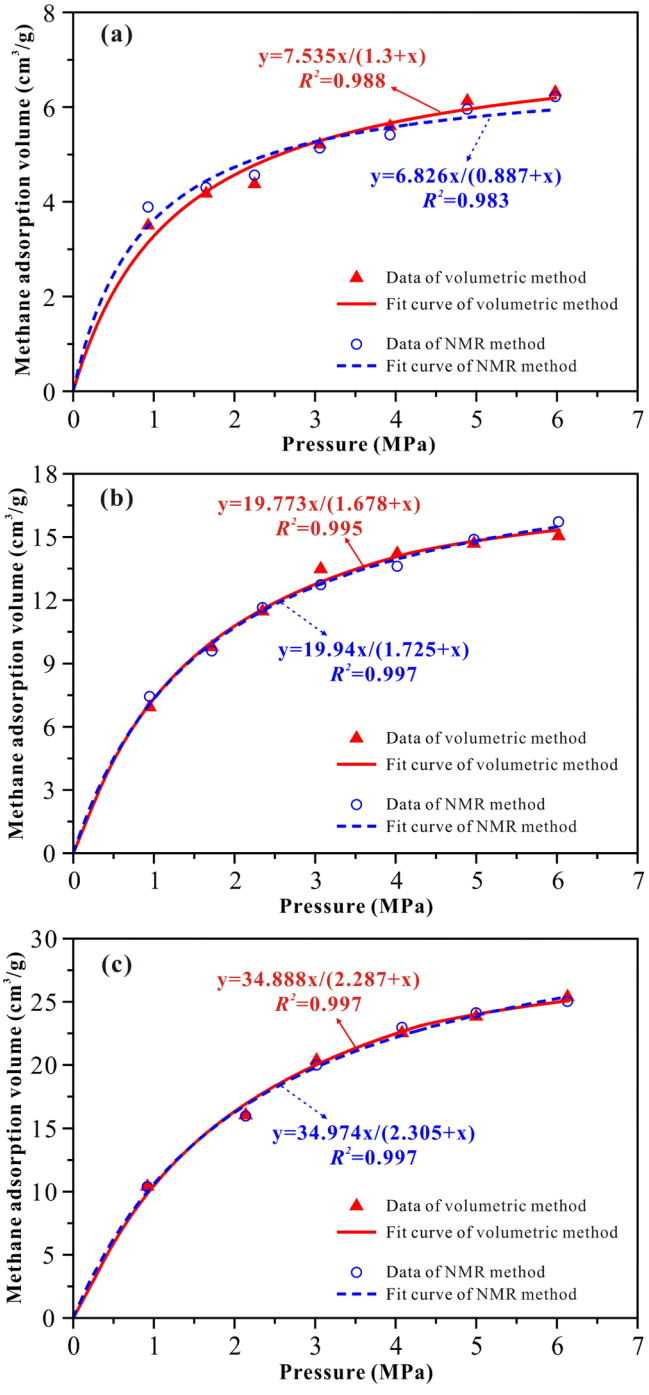

Figure 6. CH_4 isothermal adsorption curves obtained from the volumetric method and the NMR method for the LRC sample (a), MRC sample (b), and HRC sample (c).

3.3. Methane Dynamic Adsorption−Diffusion Characteristics by Low-Field NMR. *3.3.1. Dynamic Changes in T_2 Spectra during Step-By-Step Pressurization Adsorption.* During the process of step-by-step CH_4 pressurization adsorption, the dynamic change in the T_2 spectra were recorded at different time intervals. Herein, taking the times of 30, 60, 120, 180, 240, 300, and 360 min as examples, the T_2 spectral distribution of methane at different pressure steps for three coal samples is presented in Figure 7. In the initial low-pressure adsorption stage, the T_2 spectral distribution of methane significantly changes as the time increases and presents two distinct peaks or three inconspicuous peaks for coal samples (Figure 7a,d,g). Moreover, the T_2 spectra of methane are distributed at a broader relaxation time of 0.03−1000 ms and shows an obvious three-peak structure for the LRC sample during the medium−high-pressure adsorption stage (Figure 7b,c), whereas the T_2 spectral distribution of methane is almost coincident with the change in time and also has three distinct peaks within the relaxation time of 0.5−1000 ms in the medium−high-pressure adsorption stage for the MRC sample (Figure 7e,f) and the HRC sample (Figure 7h,i). These phenomena may be related to the process of methane molecules filling into pores, the adsorption effect between the methane and the pore surface in the low-pressure adsorption stage,[35,36] the slow process of further occupying the adsorption sites on the pore surface, and even the multilayered adsorption process under the van der Waals force during the medium−high-pressure adsorption stage.

Figure 8 shows the variation of the integrated T_2 amplitudes of adsorbed methane (P1 peak) and free methane (P2 and P3 peaks) in coals as a function of time at different pressurization stages. For the first pressure step of ∼1.0 MPa, the integrated T_2 amplitude of adsorbed methane increases quickly during the first 2 h (>75% of the total T_2 amplitude) and then gradually reaches the maximum value (equilibrium state) in the last 4 h for different rank coal samples (Figure 8a,c,e). As the pressure increases to ∼5.0 MPa step-by-step, the integrated T_2 amplitude of adsorbed methane has even reached more than 90% of total amplitude in 60 min. This indicates that the gas adsorption rate is very fast in the initial 1−2 h, whereas it needs a long process to reach the adsorption equilibrium state, which mainly depends on the coal properties, gas diffusion characteristics, and gas pressures. In comparison, the integrated T_2 amplitude of free methane at the first pressure step of ∼1.0 MPa significantly decreases in the first 2 h for the LRC sample (Figure 8b) and in the first hour for the MRC sample (Figure 8d), whereas there is no obvious change of that in the HRC sample during the process of step-by-step CH_4 pressurization adsorption (Figure 8f). Similarly, the integrated T_2 amplitude of free methane in LRC and MRC samples almost remained

https://dx.doi.org/10.1021/acs.energyfuels.0c03168
Energy Fuels 2020, 34, 16119−16131

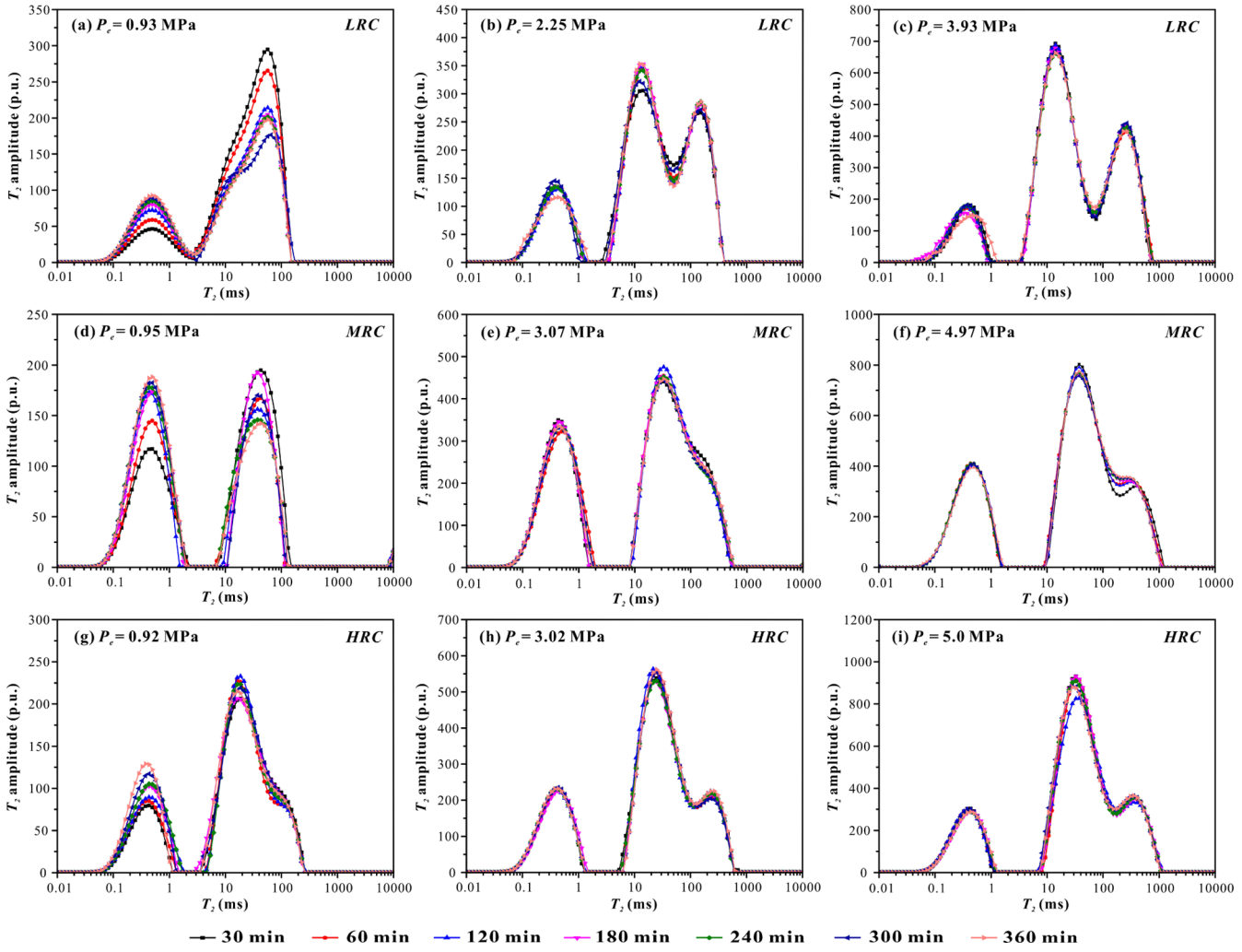

Figure 7. Representative T_2 spectral distribution at different adsorption pressures with increasing time for coal samples.

stable when the pressure gradually increases. This phenomenon may be related to the conversion rate of free methane to adsorbed methane during the adsorption process and the dynamic methane equilibrium condition between the sample cell and the reference cell. Therefore, this method can provide a fast and advanced technique to accurately analyze the CBM dynamic adsorption/desorption process at a given pressure and temperature and quantitatively identify the gas content with different existence states in coals.

3.3.2. Modeling of Methane Diffusion Process by Low-Field NMR. Based on the gas adsorption/desorption data, the unipore model, the bidisperse model, and the multiporous model are usually used to describe gas diffusion behaviors in coals, which originated from the solution to Fick's second law for spherically symmetric flow[16,17,37]

$$\frac{D}{r^2}\frac{\partial}{\partial r}\left(r^2\frac{\partial C}{\partial r}\right) = \frac{\partial C}{\partial t} \tag{10}$$

where D is the gas diffusion coefficient, r represents the pore radius, t is the time, and C is the cumulative adsorbate concentration. For a constant surface concentration of the diffusing gas, all diffusion models can be derived from eq 10 as follows

$$\frac{M_\varphi}{M_{\varphi\infty}} = 1 - \frac{6}{\pi^2}\sum_{n=1}^{\infty}\frac{1}{n^2}\exp(-D_{\varphi e}n^2\pi^2 t) \tag{11}$$

$$\frac{M_t}{M_\infty} = \sum_{\varphi=1}^{n}\frac{M_\varphi}{M_{\varphi\infty}} = \beta_1\frac{M_1}{M_{1\infty}} + \beta_2\frac{M_2}{M_{2\infty}} + \ldots + \beta_\varphi\frac{M_\varphi}{M_{\varphi\infty}} \tag{12}$$

$$\beta_1 + \beta_2 + \ldots + \beta_\varphi = 1 \tag{13}$$

where M_φ represents the amount of gas adsorbed in a certain diffusion stage at time t, $M_{\varphi n}$ is the total amount of gas adsorbed in a certain diffusion stage at indefinite time, M_t and M_∞ represent the amount of gas adsorbed at time t and the total amount of gas adsorbed at indefinite time, respectively, $D_{\varphi e}$ is the effective diffusion coefficient ($D_{\varphi e} = D/r^2$), and β_φ is the ratio of the amount of gas of certain diffusion stage to the total amount. Herein, the unipore model is equivalent to $\varphi = 1$, the bidisperse model is equivalent to $\varphi = 2$, and the multiporous model corresponds to $\varphi \geq 3$.

In this study, because of the linear relationship between the amount of adsorbed methane and the integrated T_2 amplitude of P1 peak, eqs 11−13 can be expressed by the increment in the integrated T_2 amplitude (S) at a certain pressurization step as follows

https://dx.doi.org/10.1021/acs.energyfuels.0c03168
Energy Fuels 2020, 34, 16119−16131

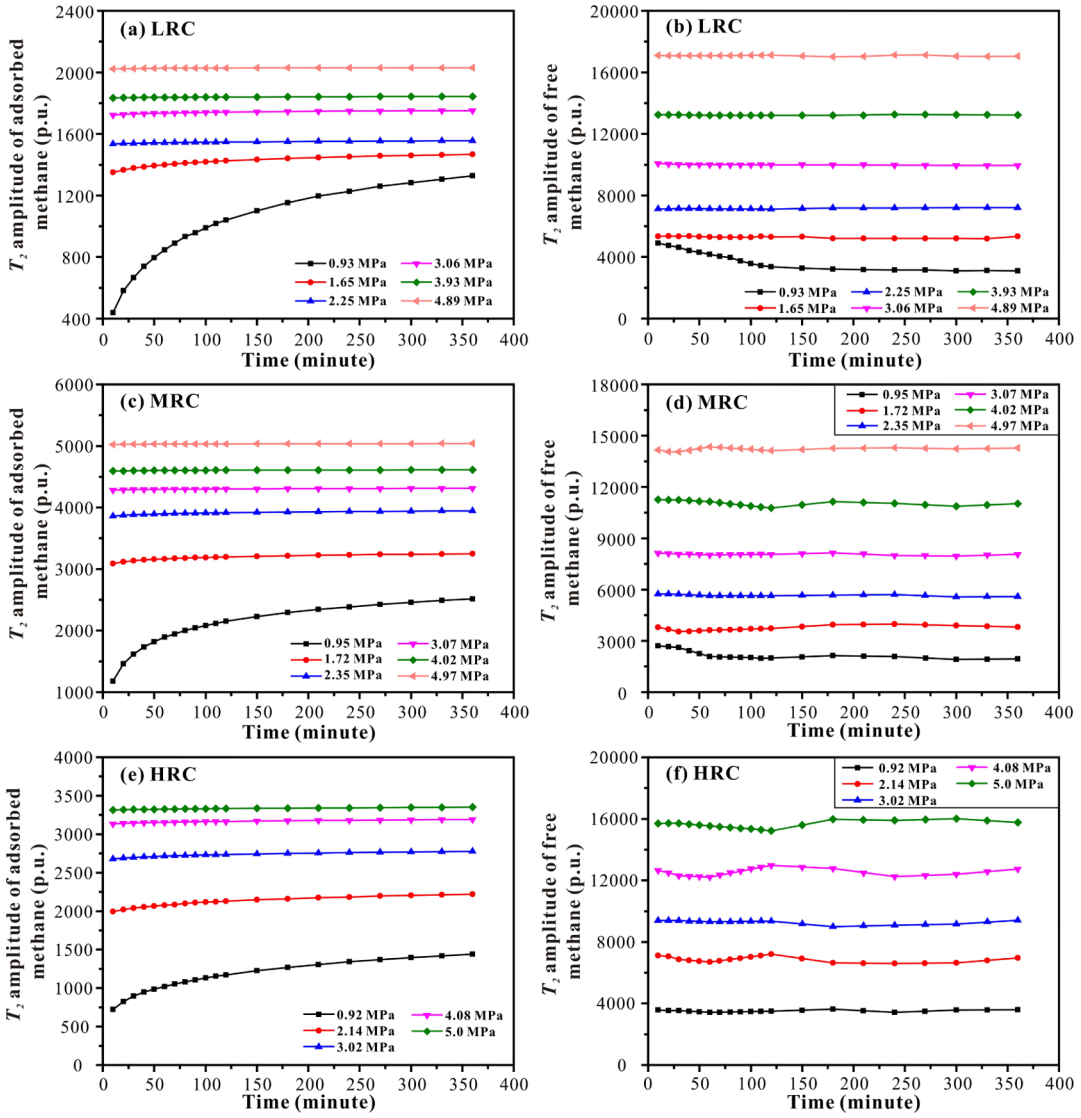

Figure 8. Dynamic change in the total T_2 amplitude of multiphase methane with respect to time at different pressures for coal samples.

$$\frac{\Delta S_{\varphi}{}^{i}}{\Delta S_{\varphi\infty}{}^{i}} = \frac{S_{\varphi}{}^{i} - S_{\infty}{}^{i-1}}{S_{\varphi\infty}{}^{i} -} = 1 - \frac{6}{\pi^2}\sum_{n=1}^{\infty}\frac{1}{n^2}\exp(-D_{\varphi e}n^2\pi^2 t) \tag{14}$$

$$\frac{\Delta S_{t}{}^{i}}{\Delta S_{\infty}{}^{i}} = \frac{S_{t}{}^{i} - S_{\infty}^{i-1}}{S_{\infty}{}^{i} - S_{\infty}{}^{i-1}} = \beta_1\frac{\Delta S_{1}{}^{i}}{\Delta S_{1\infty}{}^{i}} + \beta_2\frac{\Delta S_{2}{}^{i}}{\Delta S_{2\infty}{}^{i}} + \ldots + (1 - \beta_1 - \beta_2 - \ldots - \beta_{\varphi})\frac{\Delta S_{\varphi}{}^{i}}{\Delta S_{\varphi\infty}{}^{i}} \tag{15}$$

where i represents different CH_4 pressurization adsorption steps (i = 1−5) and the term $S_{\infty}{}^{i}$ is replaced by the integrated T_2 amplitude at 6 h for the sake of avoiding the over-parameterization. As shown in Figure 9, the adsorbed methane fraction data calculated from the integrated T_2 amplitude at different CH_4 pressurization stages as a function of time are fitted using the unipore model, the bidisperse model, and the multiporous model (φ = 3), respectively. For LRC and MRC samples, both the bidisperse model and the multiporous model agree well with the methane adsorption fraction data, and their fitting curves are almost coincident, whereas the fitting curves of unipore model obviously deviate a lot from the adsorption fraction data of different CH_4 pressurization stages (Figure 9a−f). This indicates that the methane diffusion process of LRC and MRC coals generally appears in two diffusion stages (the fast macropore diffusion stage and the slow micropore diffusion stage) or multiple diffusion stages because of the complicated bidisperse or multimodal microporous structure. Our previous research found that the bidisperse model may deviate from the data at the initial diffusion stage in some lignite samples in contrast with the multiporous model,[17] which is not evident in this work as a result of the duration limitation of the NMR signal sampling process. Moreover, the same fitting phenomenon also exists in the initial low-pressure adsorption step of 0.92 MPa for the HRC sample (Figure 9g), whereas the fitting curves of three different models tend to overlap when the methane adsorption equilibrium pressure is greater than 2.0 MPa in the HRC sample (Figure 9h,i). It suggests that the gas diffusion process of some anthracite or bright coals may present multistage characteristics during the initial low-pressure adsorption stage, and then it may change to

https://dx.doi.org/10.1021/acs.energyfuels.0c03168
Energy Fuels 2020, 34, 16119−16131

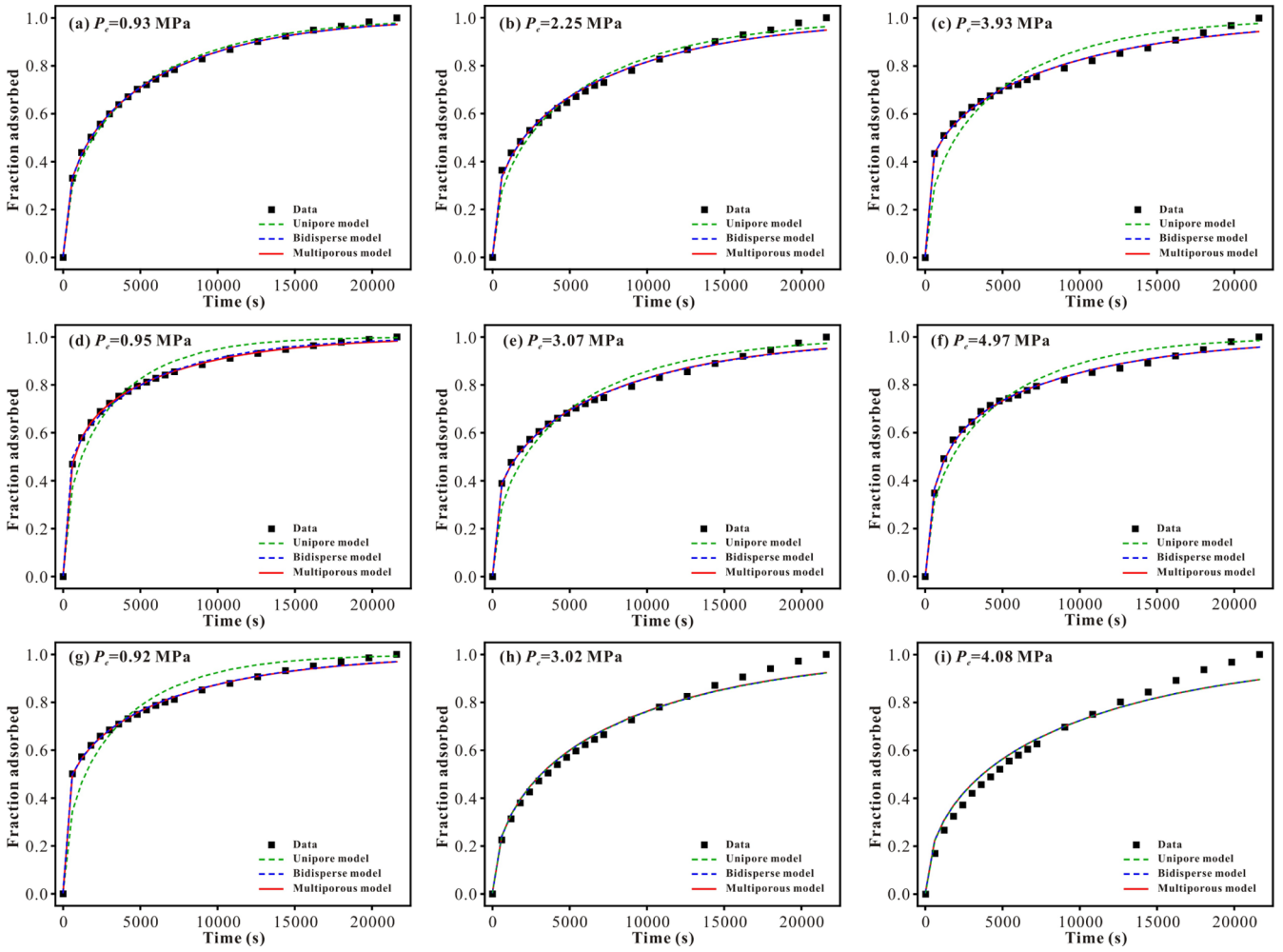

Figure 9. Representative fitting curves of the unipore model, bidisperse model, and multiporous model to the adsorbed methane fraction data calculated from the integrated T_2 amplitude of coal samples at different CH_4 pressurization stages.

the homogeneous diffusion behavior under the combined action of the complex pore structure and increasing gas pressure (the mean free path of the methane molecule) during step-by-step pressurization adsorption.[37]

3.3.3. Dynamic Changes in Diffusion Parameters during Step-By-Step Pressurization Adsorption. Through Python programing, the methane diffusion parameters and the correlation coefficient (R^2) of coal samples calculated using three diffusion models are shown in Table 3. The results indicate that the bidisperse model and the multiporous model are more suitable for describing the methane diffusion process of three coal samples (R^2 > 0.99), whereas there may be no obvious difference between the three diffusion models when the gas adsorption pressure is greater than 2.0 MPa in the HRC sample (0.904 < R^2 < 0.99). It can also be observed that the effective diffusion coefficient (D_e) of the unipore model at different pressurization adsorption steps ranges from 5.61 × 10^{-6} to 5.84 × 10^{-5} s^{-1} for three coal samples, which is between the macropore diffusion coefficient (D_{ae}) and the micropore diffusion coefficient (D_{ie}) of the bidisperse model. According to the calculation results of LRC and MRC samples, the order of magnitude of D_{ae} is approximately between 10^{-3} and 10^{-2} s^{-1} and that of D_{ie} ranges from 10^{-6} to 10^{-5} s^{-1}, which is consistent with the results of Pan et al.[16] and Wang et al.[38] As the proportion of methane adsorption amount in macropores is relatively low (0.061 <β < 0.494) in LRC and MRC samples, the D_e values are so much closer to the D_{ie} values at different pressurization adsorption steps, which indicates that the diffusion process is mainly dominated by the much slower micropore diffusion stage. Moreover, the D_{ae} of the bidisperse model generally lies between the fast diffusion coefficient (D_{fe}, 1.42−5.34 × 10^{-2} s^{-1}) and the transitional diffusion coefficient (D_{te}, 0.102−8.9 × 10^{-3} s^{-1}) of the multiporous model for LRC and MRC samples, whereas the D_{ie} is almost equal to the slow diffusion coefficient (D_{se}, 0.987−2.36 × 10^{-5} s^{-1}) of the multiporous model in this study. Meanwhile, the proportion of methane adsorption amount of fast and transitional stages (β_f and β_t) is also commensurate with that in macropores (β). Therefore, it suggests that the fast macropore diffusion process in some coals may have multistage characteristics, which are mainly controlled by the complex pore structure and distribution.

Figure 10 shows the variation of different diffusion parameters with the equilibrium pressure of coal samples during the step-by-step pressurization adsorption process. Herein, the D_e of LRC and MRC samples approximately experiences the process of decreasing first (P_e < 3.0 MPa) and then increasing (P_e > 3.0 MPa) with increasing pressure, whereas that of HRC sample tends to decrease steadily as the adsorption pressure increases (Figure 10a). This phenomenon

https://dx.doi.org/10.1021/acs.energyfuels.0c03168
Energy Fuels 2020, 34, 16119−16131

Table 3. CH_4 Diffusion Parameters of Coal Samples Calculated by Different Models[a]

		Unipore model		Bidisperse model				Multiporous model					
Sample no.	P_{ei} (MPa)	D_e (s^{-1})	R^2	β	D_{ae} (s^{-1})	D_{ie} (s^{-1})	R^2	β_f	D_{fe} (s^{-1})	β_t	D_{te} (s^{-1})	D_{se} (s^{-1})	R^2
LRC	0.93	1.56×10^{-5}	0.996	0.065	1.05×10^{-2}	1.42×10^{-5}	0.998	4.08×10^{-6}	3.44×10^{-2}	0.067	4.55×10^{-4}	1.42×10^{-5}	0.998
	1.65	1.46×10^{-5}	0.993	0.061	2.0×10^{-2}	1.33×10^{-5}	0.996	0.034	4.41×10^{-2}	0.027	8.9×10^{-3}	1.33×10^{-5}	0.996
	2.25	1.31×10^{-5}	0.984	0.107	2.74×10^{-2}	1.11×10^{-5}	0.993	0.057	3.42×10^{-2}	0.05	8.28×10^{-3}	1.11×10^{-5}	0.993
	3.06	1.32×10^{-5}	0.985	0.106	1.89×10^{-2}	1.12×10^{-5}	0.993	0.056	3.48×10^{-2}	0.049	8.21×10^{-3}	1.12×10^{-5}	0.993
	3.93	1.55×10^{-5}	0.938	0.254	1.4×10^{-2}	9.87×10^{-6}	0.994	0.129	2.16×10^{-2}	0.125	8.59×10^{-4}	9.87×10^{-6}	0.994
	4.89	5.84×10^{-5}	0.949	0.494	9.52×10^{-3}	2.45×10^{-5}	0.998	0.255	1.42×10^{-2}	0.26	3.33×10^{-4}	2.36×10^{-5}	0.999
MRC	0.95	2.54×10^{-5}	0.964	0.274	1.22×10^{-2}	1.63×10^{-5}	0.998	0.036	2.51×10^{-2}	0.303	1.83×10^{-4}	1.47×10^{-5}	0.999
	1.72	2.18×10^{-5}	0.961	0.263	2.51×10^{-2}	1.42×10^{-5}	0.998	0.132	5.34×10^{-2}	0.131	4.6×10^{-3}	1.42×10^{-5}	0.998
	2.35	1.94×10^{-5}	0.966	0.23	1.47×10^{-2}	1.33×10^{-5}	0.998	0.029	2.77×10^{-2}	0.218	3.15×10^{-4}	1.3×10^{-5}	0.998
	3.07	1.48×10^{-5}	0.968	0.184	9.85×10^{-3}	1.09×10^{-5}	0.995	0.012	2.24×10^{-2}	0.173	6.36×10^{-4}	1.08×10^{-5}	0.995
	4.02	2.8×10^{-5}	0.987	0.183	8.93×10^{-3}	2.17×10^{-5}	0.999	4.67×10^{-4}	2.06×10^{-2}	0.234	2.1×10^{-4}	2.04×10^{-5}	0.999
	4.97	1.73×10^{-5}	0.971	0.18	6.26×10^{-3}	1.29×10^{-5}	0.99	1.05×10^{-10}	1.71×10^{-2}	0.294	1.02×10^{-4}	1.09×10^{-5}	0.995
HRC	0.92	2.13×10^{-5}	0.934	0.314	1.43×10^{-2}	1.23×10^{-5}	0.997	0.127	2.31×10^{-2}	0.187	4.67×10^{-3}	1.23×10^{-5}	0.997
	2.14	1.05×10^{-5}	0.99	0.003	1.05×10^{-5}	1.05×10^{-5}	0.99	0.003	1.07×10^{-5}	0.002	1.05×10^{-5}	1.05×10^{-5}	0.99
	3.02	9.67×10^{-6}	0.986	0.006	9.67×10^{-6}	9.67×10^{-6}	0.986	0.015	9.67×10^{-6}	0.013	9.67×10^{-6}	9.67×10^{-6}	0.986
	4.08	8.27×10^{-6}	0.969	0.005	8.28×10^{-6}	8.27×10^{-6}	0.969	0.042	8.28×10^{-6}	0.042	8.27×10^{-6}	8.27×10^{-6}	0.969
	5.0	5.61×10^{-6}	0.904	0.004	5.61×10^{-6}	5.61×10^{-6}	0.904	0.008	5.62×10^{-6}	0.008	5.62×10^{-6}	5.61×10^{-6}	0.904

[a]*Note:* D_e - effective diffusion coefficient of the unipore model, D_{ae} - effective macropore diffusion coefficient of the bidisperse model, D_{ie} - effective micropore diffusion coefficient of the bidisperse model, D_{fe} - effective fast diffusion coefficient of the multiporous model, D_{te} - effective transitional diffusion coefficient of the multiporous model, and D_{se} - effective slow diffusion coefficient of the multiporous model.

https://dx.doi.org/10.1021/acs.energyfuels.0c03168
Energy Fuels 2020, 34, 16119−16131

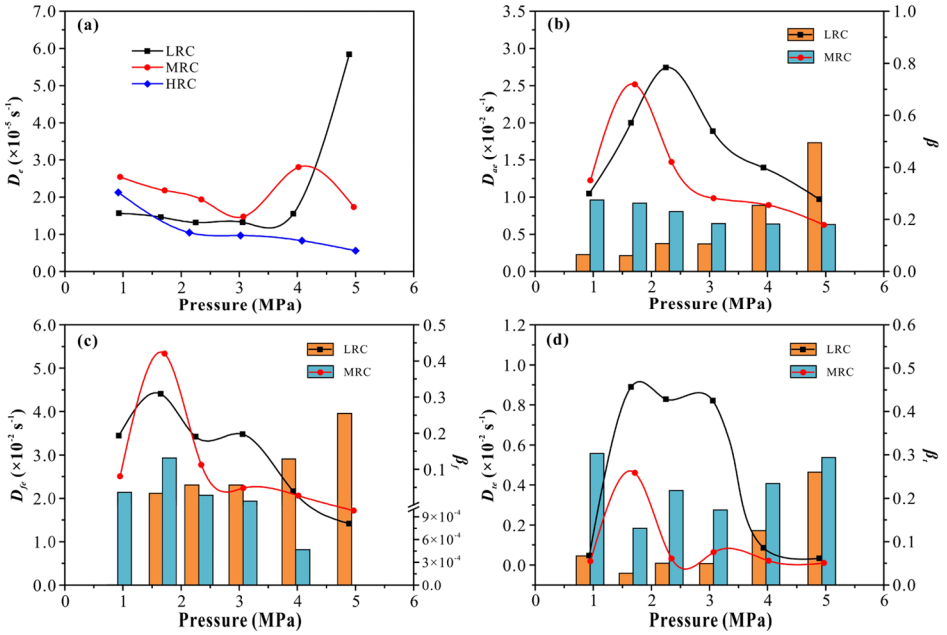

Figure 10. Relationships between the adsorption pressure and different diffusion parameters calculated from different models for coal samples.

may be related to the comprehensive effects of methane diffusion mechanisms under different adsorption pressures and coal matrix swelling during the adsorption process. On one hand, gas adsorption-induced coal matrix swelling can also be described using a Langmuir-like equation with increasing gas pressure, and its ratio is closely related to the adsorption capacity and elastic properties of coals,[39,40] which results in the reduction of pore size and even the closure of partial micropores of coals. It further leads to the decrease of methane diffusion capability in coals. On the other hand, three different mechanisms of gaseous methane diffusion (Fickian diffusion, transitional diffusion, and Knudsen diffusion) have been determined in coal pores with different pore sizes by means of comparing the pore size and the mean free paths of methane molecule ($\lambda = {KT}/{\sqrt{2}\pi d_0^2 P}$).[41,42] As the methane pressure increases, the Fickian diffusion (pore diameter > 10λ) and the transitional diffusion (0.1λ < pore diameter < 10λ) can further occur in the smaller pore of coals, which may result in the continual increase of methane diffusion capability. Because of the impact of the above two factors and the complex pore structure of coals, the D_{ae} of the bidisperse model for LRC and MRC samples first increases and then decreases with the increase of pressure (Figure 10b). Meanwhile, the proportion of macropore diffusion stage shows a gradual increasing trend for the LRC sample and a decreasing tendency for the MRC sample, respectively. Similarly, both D_{fe} and D_{te} values of the multiporous model for LRC and MRC samples increase first and then decrease, and finally tend to a fixed value as the pressure increases (Figure 10c,d). Therefore, the change in the low gas pressure has a great influence on the initial and middle stages of diffusion process in coals, while the slow diffusion stage is more sensitive to high pressures.

3.4. Application of This Study in CBM Reservoir Characterization. Until now, the total gas content of coal reservoir and gas adsorption/desorption behaviors has been generally determined by the on-site and laboratory canister adsorption/desorption measurements, which mainly focuses on the content of adsorbed gas in coals and its adsorption/desorption behaviors under different pressures.[8,43,44] However, it cannot accurately measure the residual gas content stored in the desorption canister and characterize the conversion process of gas in adsorbed and free states in coals. In this work, the low-field NMR method is preliminarily established to quantitatively analyze the distribution of adsorbed gas and free gas in coals during one-step or step-by-step adsorption/desorption process, which can be further used to estimate the content of multiphase gas in the on-site desorption test rather than being confined only in the laboratory. This method can accurately determine the residual gas content according to its T_2 spectral amplitude. Moreover, we also proposed an NMR-based method to calculate the gas diffusion coefficient and monitor the gas dynamic diffusion behavior in coals during the adsorption/desorption process. On this basis, the relevant data capture and calculation program can be linked to the NMR signal acquisition system and then the dynamic change in the gas diffusion coefficient can be depicted as soon as possible. To combine with the application of the low-field NMR method in the characterization of the pore structure, porosity, and permeability of coals,[45,46] the physical properties and gas microscopic characteristics of coal reservoir can be effectively characterized by low-field NMR measurements, which can provide significant implications for clarifying the gas storage/flow mechanisms in coals and the related parameters for the forecast of CBM production. However, there still needs a lot of work to ensure the extensive applicability of the NMR-based method in studying the dynamic adsorption-diffusion process of different rank core/bulk coal samples under in situ conditions.

4. CONCLUSIONS

In this study, the quantitative characterization of multiphase methane in coals and a study of the methane dynamic adsorption process were carried out using the low-field NMR method. Meanwhile, three different diffusion models were applied to study the CH_4 diffusion behaviors on the basis of integrated T_2 amplitudes with respect to different CH_4

https://dx.doi.org/10.1021/acs.energyfuels.0c03168
Energy Fuels 2020, 34, 16119−16131

pressurization stages, and the dynamic changes in diffusion parameters and their controlling mechanisms were discussed. The main conclusions are summarized as follows:

(1) The T_2 spectra of multiphase methane in a coal-filled sample cell usually exhibit two distinct peaks of adsorbed methane (P1) and porous medium-confined methane (P2) in the low-pressure adsorption stage, and another peak of bulk methane (P3) obviously appears when the pressure is greater than 2.0 MPa. The T_2 interval of P1 always falls within 0−2.5 ms, whereas the T_{2C2} between P2 and P3 is not fixed for different rank coals, which is related to the pore morphology, connectivity, and pore size distribution of coals.

(2) Both the adsorbed methane volume and the free methane volume demonstrate a strong linear correlation with their corresponding T_2 amplitude. The relative deviation of adsorbed methane volume between the volumetric method and the NMR method is less than ∼10% for the LRC sample, ∼8.0% for the MRC sample, and ∼2.0% for the HRC sample. For the first pressure step of ∼1.0 MPa, the adsorbed methane volume increases quickly during the first 2 h (>75% of total) and then gradually reaches the equilibrium state in the last 4 h, whereas it even reached more than 90% of total volume in 60 min when the pressure increased.

(3) For LRC and MRC samples, the bidisperse model and the multiporous model agree well with the integrated T_2 amplitude data at different CH_4 pressurization stages and the fitting curves of the unipore model obviously deviate a lot, whereas the fitting curves of three different models tend to overlap when the adsorption pressure is greater than 2.0 MPa in the HRC sample. The variations of CH_4 diffusion parameters with different pressures may be related to the comprehensive effects of methane diffusion mechanisms under different adsorption pressures and the coal matrix swelling during the adsorption process. Overall, the proposed NMR-based method can provide an effective technique to accurately determine the content of multiphase gas and the dynamic adsorption−diffusion process of different rank core/bulk coal samples under in situ conditions.

AUTHOR INFORMATION

Corresponding Author

Dameng Liu − *School of Energy Resources and Coal Reservoir Laboratory of National Engineering Research Center of CBM Development & Utilization, China University of Geosciences, Beijing 100083, China;* orcid.org/0000-0002-4688-074X; Phone: +86-10-82323971; Email: dmliu@cugb.edu.cn; Fax: + 86-10-82326850

Authors

Zhentao Li − *State Key Laboratory of Organic Geochemistry, Guangzhou Institute of Geochemistry, Chinese Academy of Sciences, Guangzhou 510640, China; School of Energy Resources, China University of Geosciences, Beijing 100083, China*

Songbin Xie − *Jinan Rail Transit Group Co. Ltd., Jinan 250000, China*

Xianglong Fang − *School of Energy Resources and Coal Reservoir Laboratory of National Engineering Research Center of CBM Development & Utilization, China University of Geosciences, Beijing 100083, China*

Guangyao Si − *School of Minerals and Energy Resources Engineering, University of New South Wales, Sydney 2052, NSW, Australia*

Yidong Cai − *School of Energy Resources and Coal Reservoir Laboratory of National Engineering Research Center of CBM Development & Utilization, China University of Geosciences, Beijing 100083, China;* orcid.org/0000-0002-4915-5615

Yunpeng Wang − *State Key Laboratory of Organic Geochemistry, Guangzhou Institute of Geochemistry, Chinese Academy of Sciences, Guangzhou 510640, China;* orcid.org/0000-0003-4164-9677

Complete contact information is available at: https://pubs.acs.org/10.1021/acs.energyfuels.0c03168

Notes

The authors declare no competing financial interest.

ACKNOWLEDGMENTS

This research was funded by the National Natural Science Foundation of China (grant nos. 41902165, 41922016, 41830427, and 41772160), the International Postdoctoral Exchange Fellowship Program from China Postdoctoral Council (grant no. 20190070), the Project funded by China Postdoctoral Science Foundation (grant no. 2018M643222), Strategic Priority Research Program of the Chinese Academy of Sciences (XDA14010103), and China National Major S&T Program (2017ZX05008-002-030).

REFERENCES

(1) Lau, H. C.; Li, H.; Huang, S. Challenges and opportunities of coalbed methane development in China. *Energy Fuels* **2017**, *31*, 4588−4602.

(2) Zhang, D.; Liu, S.; Fu, X.; Jia, S.; Min, C.; Pan, Z. Adsorption and desorption behaviors of nitrous oxide on various rank coals: implications for oxy-coal combustion flue gas sequestration in deep coal seams. *Energy Fuels* **2019**, *33*, 11494−11506.

(3) Lupton, N.; Connell, L. D.; Heryanto, D.; Sander, R.; Camilleri, M.; Down, D. I.; Pan, Z. Enhancing biogenic methane generation in coalbed methane reservoirs - Core flooding experiments on coals at in-situ conditions. *Int. J. Coal Geol.* **2020**, *219*, 103377.

(4) Nie, B. S.; He, X. Q.; Wang, E. Y. Mechanism and modes of gas diffusion in coal seams. *China Saf. Sci. J.* **2000**, *10*, 24−28.

(5) Pillalamarry, M.; Harpalani, S.; Liu, S. Gas diffusion behavior of coal and its impact on production from coalbed methane reservoirs. *Int. J. Coal Geol.* **2011**, *86*, 342−348.

(6) Karacan, C. Ö.; Okandan, E. Assessment of energetic heterogeneity of coals for gas adsorption and its effect on mixture predictions for coalbed methane studies. *Fuel* **2000**, *79*, 1963−1974.

(7) Li, X.; Fu, X.; Liu, A.; An, H.; Wang, G.; Yang, X.; Wang, L.; Wang, H. Methane adsorption characteristics and adsorbed gas content of low-rank coal in China. *Energy Fuels* **2016**, *30*, 3840−3848.

(8) Li, J.; Lu, S.; Zhang, P.; Cai, J.; Li, W.; Wang, S.; Feng, W. Estimation of gas-in-place content in coal and shale reservoirs: A process analysis method and its preliminary application. *Fuel* **2020**, *259*, 116266.

(9) Busch, A.; Gensterblum, Y. CBM and CO2-ECBM related sorption processes in coal: A review. *Int. J. Coal Geol.* **2011**, *87*, 49−71.

(10) Cai, Y.; Liu, D.; Pan, Z.; Yao, Y.; Li, J.; Qiu, Y. Pore structure and its impact on CH4 adsorption capacity and flow capability of bituminous and subbituminous coals from Northeast China. *Fuel* **2013**, *103*, 258−268.

(11) Chalmers, G. R. L.; Marc Bustin, R. On the effects of petrographic composition on coalbed methane sorption. *Int. J. Coal Geol.* **2007**, *69*, 288−304.

(12) Gensterblum, Y.; Merkel, A.; Busch, A.; Krooss, B. M. High-pressure CH4 and CO2 sorption isotherms as a function of coal maturity and the influence of moisture. *Int. J. Coal Geol.* **2013**, *118*, 45−57.
(13) Hou, H.; Shao, L.; Li, Y.; Li, Z.; Wang, S.; Zhang, W.; Wang, X. Influence of coal petrology on methane adsorption capacity of the Middle Jurassic coal in the Yuqia Coalfield, northern Qaidam Basin, China. *J. Pet. Sci. Eng.* **2017**, *149*, 218−227.
(14) Chen, D.; Ye, Z.; Pan, Z.; Tan, Y.; Li, H. Theoretical models to predict gas adsorption capacity on moist coal. *Energy Fuels* **2019**, *33*, 2908−2914.
(15) Zhu, C.-j.; Ren, J.; Wan, J.; Lin, B.-q.; Yang, K.; Li, Y. Methane adsorption on coals with different coal rank under elevated temperature and pressure. *Fuel* **2019**, *254*, 115686.
(16) Pan, Z.; Connell, L. D.; Camilleri, M.; Connelly, L. Effects of matrix moisture on gas diffusion and flow in coal. *Fuel* **2010**, *89*, 3207−3217.
(17) Li, Z.; Liu, D.; Cai, Y.; Shi, Y. Investigation of methane diffusion in low-rank coals by a multiporous diffusion model. *J. Nat. Gas Sci. Eng.* **2016**, *33*, 97−107.
(18) Yao, Y.; Liu, D. Comparison of low-field NMR and mercury intrusion porosimetry in characterizing pore size distributions of coals. *Fuel* **2012**, *95*, 152−158.
(19) Zhao, Y.; Zhu, G.; Dong, Y.; Danesh, N. N.; Chen, Z.; Zhang, T. Comparison of low-field NMR and microfocus X-ray computed tomography in fractal characterization of pores in artificial cores. *Fuel* **2017**, *210*, 217−226.
(20) Korb, J.-P.; Nicot, B.; Jolivet, I. Dynamics and wettability of petroleum fluids in shale oil probed by 2D T 1 -T 2 and fast field cycling NMR relaxation. *Microporous Mesoporous Mater.* **2018**, *269*, 7−11.
(21) Sun, X.; Yao, Y.; Liu, D.; Zhou, Y. Investigations of CO2-water wettability of coal: NMR relaxation method. *Int. J. Coal Geol.* **2018**, *188*, 38−50.
(22) Li, X.; Fu, X.; Ranjith, P. G.; Xu, J. Stress sensitivity of medium- and high volatile bituminous coal: An experimental study based on nuclear magnetic resonance and permeability-porosity tests. *J. Pet. Sci. Eng.* **2019**, *172*, 889−910.
(23) Liu, Z.; Liu, D.; Cai, Y.; Yao, Y.; Pan, Z.; Zhou, Y. Application of nuclear magnetic resonance (NMR) in coalbed methane and shale reservoirs: A review. *Int. J. Coal Geol.* **2020**, *218*, 103261.
(24) Alexeev, A. D.; Vasylenko, T. A.; Ul'yanova, E. V. Phase states of methane in fossil coals. *Solid State Commun.* **2004**, *130*, 669−673.
(25) Guo, R.; Mannhardt, K.; Kantzas, A. Characterizing moisture and gas content of coal by low-field NMR. *J. Can. Pet. Technol.* **2007**, *46*, 49−54.
(26) Yao, Y.; Liu, D.; Xie, S. Quantitative characterization of methane adsorption on coal using a low-field NMR relaxation method. *Int. J. Coal Geol.* **2014**, *131*, 32−40.
(27) Yao, Y.; Liu, J.; Liu, D.; Chen, J.; Pan, Z. A new application of NMR in characterization of multiphase methane and adsorption capacity of shale. *Int. J. Coal Geol.* **2019**, *201*, 76−85.
(28) Liu, X.; Wu, C. Simulation of dynamic changes of methane state based on NMR during coalbed methane output. *Fuel* **2017**, *194*, 188−194.
(29) Zhang, J.; Wei, C.; Vandeginste, V.; Ju, W.; Qin, Z.; Quan, F.; Soh Tamehe, L. Experimental simulation study on water migration and methane depressurizing desorption based on nuclear magnetic resonance technology: A case study of middle-rank coals from the Panguan syncline in the western Guizhou region. *Energy Fuels* **2019**, *33*, 7993−8006.
(30) Wang, F.; Yao, Y.; Wen, Z.; Sun, Q.; Yuan, X. Effect of water occurrences on methane adsorption capacity of coal: A comparison between bituminous coal and anthracite coal. *Fuel* **2020**, *266*, 117102.
(31) Zhao, G.; Wang, C. Influence of CO2 on the adsorption of CH4 on shale using low-field nuclear magnetic resonance technique. *Fuel* **2019**, *238*, 51−58.
(32) Liu, J.; Xie, L.; Yao, Y.; Gan, Q.; Zhao, P.; Du, L. Preliminary study of influence factors and estimation model of the enhanced gas recovery stimulated by carbon dioxide utilization in shale. *ACS Sustainable Chem. Eng.* **2019**, *7*, 20114−20125.
(33) Quan, F.; Wei, C.; Zhang, J.; Feng, S.; Hao, S.; Lu, G.; Hu, Y. Study on desorption and diffusion dynamics of coal reservoir through step-by-step depressurization simulation–an experimental simulation study based on LF-NMR technology. *J. Nat. Gas Sci. Eng.* **2020**, *75*, 103149.
(34) Zheng, S.; Yao, Y.; Elsworth, D.; Liu, D.; Cai, Y. Dynamic Fluid Interactions during CO2-Enhanced Coalbed Methane and CO2 Sequestration in Coal Seams. Part 1: CO2-CH4 Interactions. *Energy Fuels* **2020**, *34*, 8274−8282.
(35) Sang, S. X.; Zhu, Y. M.; Zhang, J.; Zhang, X. D.; Tang, J. X. Solid-gas interaction mechanism of coal-adsorbed gas (II) - physical process and theoretical model of coal-adsored gas. *Nat. Gas Ind.* **2005**, *25*, 16−21. (in Chinese)
(36) Karacan, C.; Okandan, E. Adsorption and gas transport in coal microstructure: investigation and evaluation by quantitative X-ray CT imaging. *Fuel* **2001**, *80*, 509−520.
(37) Clarkson, C. R.; Bustin, R. M. The effect of pore structure and gas pressure upon the transport properties of coal: a laboratory and modeling study. 2. Adsorption rate modeling. *Fuel* **1999**, *78*, 1345−1362.
(38) Wang, K.; Zang, J.; Feng, Y.; Wu, Y. Effects of moisture on diffusion kinetics in Chinese coals during methane desorption. *J. Nat. Gas Sci. Eng.* **2014**, *21*, 1005−1014.
(39) Robertson, E. P.; Christiansen, R. L. Measurement of sorption-induced strain. *2005 International Coalbed Methane Symposium*; Tuscaloosa: Alabama, 2005; pp 17−19 May. Paper 0532.
(40) Pan, Z.; Connell, L. D. A theoretical model for gas adsorption-induced coal swelling. *Int. J. Coal Geol.* **2007**, *69*, 243−252.
(41) Reeves, S.; Pekot, L. Advanced reservoir modeling in desorption-controlled reservoirs. In: *SPE Rocky Mountain Petroleum Technology Conference*. SPE, Keystone, Colorado, 2001, pp. 21-23.
(42) Xu, H.; Tang, D.; Zhao, J.; Li, S.; Tao, S. A new laboratory method for accurate measurement of the methane diffusion coefficient and its influencing factors in the coal matrix. *Fuel* **2015**, *158*, 239−247.
(43) Bustin, A. M. M.; Bustin, R. M. Total gas-in-place, gas composition and reservoir properties of coal of the Mannville coal measures, Central Alberta. *Int. J. Coal Geol.* **2016**, *153*, 127−143.
(44) Pan, J.; Lv, M.; Hou, Q.; Han, Y.; Wang, K. Coal microcrystalline structural changes related to methane adsorption/desorption. *Fuel* **2019**, *239*, 13−23.
(45) Zheng, S.; Yao, Y.; Liu, D.; Cai, Y.; Liu, Y. Characterizations of full-scale pore size distribution, porosity and permeability of coals: A novel methodology by nuclear magnetic resonance and fractal analysis theory. *Int. J. Coal Geol.* **2018**, *196*, 148−158.
(46) Liu, Z.; Wang, W.; Cheng, W.; Yang, H.; Zhao, D. Study on the seepage characteristics of coal based on the Kozeny-Carman equation and nuclear magnetic resonance experiment. *Fuel* **2020**, *266*, 117088.

https://dx.doi.org/10.1021/acs.energyfuels.0c03168
Energy Fuels 2020, 34, 16119−16131